Memory effect in a ferroelectric single-electron transistor: Violation of conductance periodicity in the gate voltage

S. A. Fedorov,[1,2] A. E. Korolkov,[1,2] N. M. Chtchelkatchev,[1,3,4] O. G. Udalov,[3,5] and I. S. Beloborodov[3]

[1]*Department of Theoretical Physics, Moscow Institute of Physics and Technology, Moscow 141700, Russia*

[2]*P.N. Lebedev Physical Institute of the Russian Academy of Sciences, Moscow 119991, Russia*

[3]*Department of Physics and Astronomy, California State University Northridge, Northridge, California 91330, USA*

[4]*L.D. Landau Institute for Theoretical Physics, Russian Academy of Sciences, Moscow 117940, Russia*

[5]*Institute for Physics of Microstructures, Russian Academy of Science, Nizhny Novgorod, 603950, Russia*

(Received 27 August 2014; revised manuscript received 20 October 2014; published 7 November 2014)

A fundamental property of most single-electron devices with a quasicontinuous quasiparticle spectrum on an island is the periodicity of their transport characteristics in a gate voltage. This property is robust even with respect to placing ferroelectric insulators in the source and drain tunnel junctions. We show that placing a ferroelectric insulator inside the gate capacitance breaks this periodicity. The current-voltage characteristics of this single-electron transistor strongly depends on the ferroelectric polarization and shows a giant memory effect even for negligible ferroelectric hysteresis making this device promising for memory applications.

DOI: 10.1103/PhysRevB.90.195111 PACS number(s): 77.80.−e, 72.80.Tm, 77.84.Lf

I. INTRODUCTION

Ferroelectricity like magnetism has been under investigation for decades. Recent progress in ferroelectricity is stimulated by (i) the miniaturization of ferroelectric samples to the nanoscale where they show new physical properties compared to the bulk ferroelectric materials [1–14], and (ii) modern computer processors and memory demand storing, where moving electric charges and controlling the associated electric fields is important. There is a tendency for further increase of computer efficiency that results in facing the nanolevel with individual electrons and atoms. In ferroelectric materials, polarization is produced by atom displacements. Nanoferroelectrics combined with single-electron nanocircuits are thus promising devices for memory storage and information processing.

Recently, it was shown that the presence of ferroelectricity in the source and drain tunnel junctions of a single-electron transistor (SET), see Fig. 1, induces a memory effect in the current-voltage characteristics even in the limit of negligible hysteresis of the ferroelectric insulators [15]. The bottleneck of ferroelectric SET is the experimental difficulty to produce ultrathin and ultrasmall ferroelectric tunnel junctions with special parameters. Technologically it is much easier to produce a nanothin ferroelectric layer but not thin enough for perfect electron tunneling. Such a layer can be placed into the gate capacitance of the SET. At first glance, the physics of a such ferroelectric should be similar to the physics of SET considered in Ref. [15] with a ferroelectric source and drain capacitors, however, this is not so.

A fundamental property of most single-electron devices with a quasicontinuous quasiparticle spectrum on an island is the periodicity of their transport characteristics in a gate voltage. This property is robust even with respect to placing ferroelectric insulators in the source and drain tunnel junctions [15]. We show that placing the ferroelectric inside the gate capacitance breaks this periodicity even for negligible ferroelectric hysteresis. Applying a relatively small "switching" gate voltage one can change the polarization of the ferroelectric material. We show that further increase of the gate voltage does not affect the direction of the ferroelectric polarization. The current-voltage characteristics of this SET strongly depends on the ferroelectric polarization and shows a memory effect making this device promising for memory applications.

II. SINGLE-ELECTRON TRANSISTOR WITH FERROELECTRIC GATE

A. The model

The ferroelectricity localized in the gate capacitance changes the distribution of the excess charge in the nanograin. In the absence of quantum fluctuations the grain charge is $ne = \sum_i \{C_i[\phi(n) - V_i]\} + \int_g d\mathbf{S}_g \cdot \mathbf{P}_g$. Here, n is the excess charge number, e is the elementary charge, $\phi(n)$ is the potential of the nanograin, C_i with $i = 1,2,g$ are the capacitances, and $\mathbf{S}_g$ is the grain surface. The surface integration is performed over the nanograin part, which is in contact with the ferroelectric. The polarization $\mathbf{P}_g$ itself depends on the grain charge. Thus calculations of the charge statistics and polarization should be done self-consistently [15].

Generally, the electric field dependence of polarization in SET has hysteresis. The following model takes this effect into account:

$$P^{(u/d)}(\mathcal{E}) = P^0 \tanh\left(\frac{\mathcal{E} \pm \mathcal{E}_h}{\mathcal{E}_s}\right) + \alpha\mathcal{E}, \qquad (1)$$

where "u" and "d" stands for the upper and lower branches of hysteresis loop, $\mathcal{E}_s$ is the saturation field, P^0 is the saturation polarization amplitude, and $\mathcal{E}_h$ describes the width of the hysteresis loop. Similarly, we can write the voltage dependence of the polarization introducing $V_s = \mathcal{E}_s d$ and $V_h = \mathcal{E}_h d$, where d is the width of the gate capacitor: $P^{(u/d)}(V) = P^0 \tanh(\frac{V \pm V_h}{V_s}) + \alpha V$. The typical graph of $P(V)$ is shown in Fig. 2.

In typical single-electron devices the electron tunneling is a much faster process than the relaxation of the ferroelectric [15]. This is related to the fact that ferroelectricity is related to the shift of ions that are heavy and inert. Therefore the ferroelectric in SET is sensitive to the average electric field

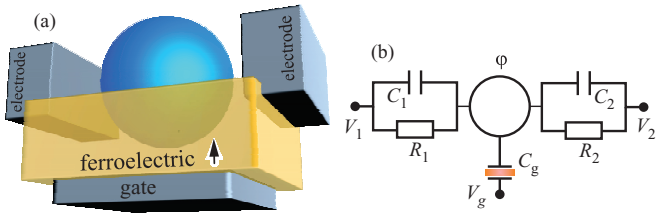

FIG. 1. (Color online) (a) Sketch of a single-electron transistor (SET) with a ferroelectric placed at the gate capacitor. (b) The equivalent scheme.

over the "fast" electron-tunneling events [15]. Thus, for a fixed ferroelectric polarization **P**, we can calculate the average grain potential $\langle\phi\rangle$. Since $\langle\phi\rangle$ itself depends on the polarization P through the probability distribution $p(n)$, to find n excess charges on the grain, we obtain the self-consistency equation. The probabilities can be calculated using the modified SET orthodox theory, see Refs. [15–18], where self-consistency was developed for an SET with a slowly oscillating gate electrode.

B. Dimensionless units and basic notations

An SET has a number of important parameters. It is convenient to use the following units for analytical and numerical calculations: $2E_c = e^2/C_\Sigma$ is the energy and temperature unit ($k_B = 1$), the elementary charge e is the charge-unit (electron charge is equal -1). The capacitance becomes dimensionless using $e^2/2E_c$, so $C_\Sigma = 1$. We use the (bare) tunneling resistance of the first tunnel junction, R_1, between the left electrode and the nanograin as the unit for the resistance. Also we use the effective gate charge as a control parameter, $Q_0 = -V_g C_g$.

III. FERROELECTRIC SET AT LOW TEMPERATURES ORTHODOX THEORY

Here, we consider the limit of low temperatures, $T \ll E_c$ where the transport properties of an SET (not far from the degeneracy points) are well described by the "orthodox model" [19–22]. Generalization of the orthodox model for an SET with ferroelectricity was recently formulated in Ref. [15]. Using the equations of Ref. [15], one can find the distribution functions $p(n)$ describing the excess charge statistics on the grain, the mutual dependence of ferroelectric polarization, the charge statistics, and the electron current.

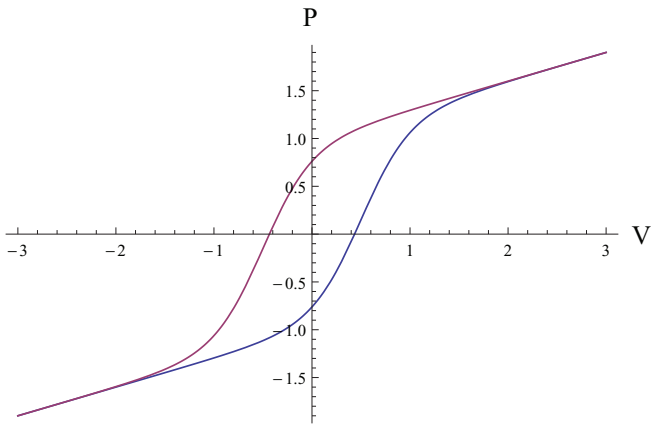

FIG. 2. (Color online) Model polarization.

A. Ferroelectric with ultrathin hysteresis loop

First, we consider the limiting case of an ultrathin ferroelectric hysteresis loop, with $\mathcal{E}_h = 0$ in Eq. (1). Also, we assume that the parameter $\alpha = 0$ in Eq. (1). Using these assumptions, we explain the strong influence of ferroelectricity in the gate capacitor on a fundamental property of SET, the periodicity of its transport properties in a gate voltage V_g.

1. *Ferroelectric with small switching field:* $V_s \ll 1$

The basic features of an SET with ferroelectricity in the gate capacitor can be qualitatively understood for a small switching field, $V_s \ll 1$. First, we investigate the SET for zero driving voltage, $V = 0$, and zero switching voltage, $V_s = 0$. We also assume that electrons do not hop between the leads and the grain. This assumption is reasonable for gate voltages away from the points of intersection of different free energy branches. In this case, the charge number on the grain does not fluctuate and the average potential is equal to the instant potential $\phi = \langle\phi\rangle$ and $\int_g \mathbf{P}\cdot d\mathbf{S}_g = q_0\,\mathrm{sign}(\phi - V_g)$. The equation describing the potential ϕ has the form

$$ne = C\phi + C_g(\phi - V_g) + q_0\,\mathrm{sign}(\phi - V_g). \tag{2}$$

Here, $C = C_1 + C_2$. Equation (2) has the following solution in the limit $V_s \to 0$:

$$\phi = \begin{cases} \frac{C_g V_g + ne + q_0}{C + C_g}, & V_g > \frac{ne+q_0}{C}, \\ \frac{C_g V_g + ne - q_0}{C + C_g}, & V_g < \frac{ne-q_0}{C}, \\ V_g, & \frac{ne-q_0}{C} < V_g < \frac{ne+q_0}{C}. \end{cases} \tag{3}$$

Each branch of potential ϕ has three regions. Two regions have the same slope but they are shifted by a voltage $2q_0/C_\Sigma$. The transition between these regions is located in the vicinity of the point $Q_0 = -C_g ne/C$ with the width of $C_g 2q_0/C$. For a parameter $q_0 < 0.5e$, the different branches do not intersect each other, while for $q_0 > 0.5e$ the branches intersect each other on the line $\phi = -Q_0/C_g$. The intersection of ϕ with 0 is happening at the point $(ne \pm q_0)$.

Following the orthodox theory, we introduce the effective free energy of the SET:

$$F = \min_n f_n,\ f_n = E_c(C_\Sigma\phi)^2 = E_c(en - Q_0 - P)^2. \tag{4}$$

For zero polarization, $P = 0$, the function f_n is a parabola in the parameter $Q_0 = -V_g C_g$. At finite P, the ferroelectric polarization depends on the parameter Q_0 making the function $f_n(Q_0)$ a more complicated function consisting of parabola fragments separated by a transition region, see Fig. 3. At the degeneracy points, where the functions $f_n(Q_0)$ intersect, the Coulomb blockade is suppressed allowing electrons to go through the SET from one lead to another. The positions of these degeneracy points, corresponding to the conductivity maxima, are $[(n + 1/2)e \pm q_0]$. Thus all the conductivity peaks move to the zero gate voltage point. If a peak reaches the point $Q_0 = 0$, it stays at this point with further increase of parameter q_0. All peaks have the same shift magnitude, but the direction is different for peaks below and above the point

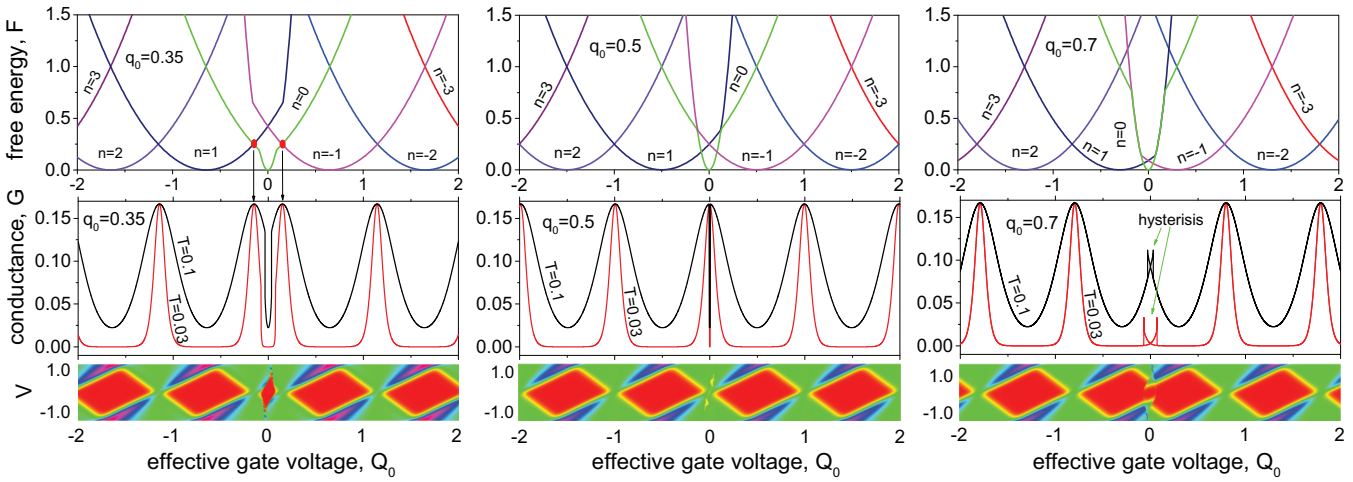

FIG. 3. (Color online) Ferroelectricity breaks down a fundamental property of an SET: the periodicity of its transport properties in a gate voltage V_g. Only for an effective gate voltage $|Q_0| > 1/2$ the conductance peaks are equidistant. Upper row: the effective free energy f_n of an SET, see Eq. (4). Middle raw: the zero bias conductance. Lower raw: the conductance density plot. Parameters: $C_1 = 0.3$, $C_2 = 0.5$, $C_g = 0.2$, $R_1 = 1$, $R_2 = 2$, $V_s = 0.01$, and $V_h = 0$.

$Q_0 = 0$. This leads to the breaking of periodicity in the conductivity peaks of FE SET. The numerically calculated conductance peaks approximately correspond to the degeneracy points as shown in Fig. 3.

In orthodox theory, the conductance of SET (without ferroelectricity) at low temperatures, $T \ll E_c$, is

$$G(\delta Q_0) = \frac{1}{2}\,\frac{1}{R_1 + R_2}\,\frac{e\,\delta Q_0/C_\Sigma T}{\sinh(e\,\delta Q_0/C_\Sigma T)}. \qquad (5)$$

Here, $\delta Q_0 = \min_k[Q_0 - (2k+1)\frac{e}{2}] \ll e$ is the deviation of the induced charge by the gate terminal from the nearest degeneracy point. With ferroelectricity in the gate, we should replace the deviation δQ_0 by

$$\delta Q_s \to \min_k \left[q_0 \tanh\left(\frac{\langle\phi\rangle + Q_0/C_g}{V_s}\right) + Q_0 - (2k+1)\frac{e}{2}\right]. \qquad (6)$$

This equation is valid for a small parameter $q_0 \ll 1$. For small switching voltage, $V_s \lesssim 1$, we can replace tanh in Eq. (6) by unity and using Eq. (5) find that the conductance peaks are shifted by q_0 for $Q_0 > 0$ and by $-q_0$ for $Q_0 < 0$. This is consistent with numerical calculations, see Fig. 3.

The most important effect that follows from Eq. (6) in the presence of a ferroelectric material is the break up of conductance periodicity in the parameter Q_0. This periodicity is the basic property of SETs; it is robust in the presence of ferroelectrics in the capacitors between the left and the right leads [15]. However, numerical calculations show that this periodicity is absent when a ferroelectric is placed inside the gate capacitor, see Fig. 3.

This break of periodicity is a very general result. It follows from the nonperiodic and nonlinear dependence of the FE polarization on the effective charge Q_0. The FE polarization is defined by the difference of two quantities, the average grain potential $\langle\phi\rangle$ and the gate voltage V_g. The potential $\langle\phi\rangle$ oscillates around zero while the voltage V_g grows unlimited. As a result, the FE polarization is saturated for voltages $|V_g| \gg |e|/C_\Sigma + V_s$, however, its direction depends on the sign of the gate voltage V_g producing the opposite shifts of conductance peaks at voltages $V_g = \pm\infty$.

Another interesting phenomenon appearing due to the presence of the FE layer is the hysteresis conductivity behavior. We remind that in this section we consider an FE without hysteresis. However, even in this case, the conductivity peak in the vicinity of $Q_0 = 0$ is split into two branches, see the right panel in Fig. 3. The pronounced [23] hysteresis appears for $q_0 > 0.5$ where the system polarization has two stable ground states corresponding to two different directions of the FE polarization (toward the grain and toward the gate) and two different grain charges, positive and negative. These two states have different conductivity. For steplike polarization, the hysteresis appears for peaks located in the vicinity of $Q_0 = 0$.

With increasing temperature the hysteresis disappears. The criterion for hysteresis existence has the form, $e\Gamma_{0,1}/(\Gamma_{0,1} + \Gamma_{1,0}) = Q_{\max} < q_0$, where $\Gamma_{i,j}$ is the transition rate between the states with grain charges i and j and $0.5 < q_0 < 1.5$. $Q_{\max}$ decreases with increasing temperature. We demonstrate the existence of two ground states in the Appendix A 5.

Now we consider small but finite values of switching voltage V_s and investigate the correlation of the conductance peaks and polarization evolution with parameter Q_0. For a parameter $q_0 \leqslant 0.5$, the conductance peaks do not merge, however, they deform approaching the point $Q_0 = 0$. This is related to the switching of polarization with Q_0, see Fig. 4.

For $0.5 < q_0 < 1$, the conductance shows a pronounced memory effect (hysteresis), Fig. 3. The positions of the jumps in the conductance correspond to the divergences of $\frac{dG}{dQ_0}$ [15]. The amplitude of the conductance peaks in this regime is suppressed for $q_0 > T$. The evolution of memory effect in the conductance with parameter q_0 is shown in Fig. 3. The conductance has similar behavior for $1 < q_0 < 1.5$ and for $1.5 < q_0 < 2$ its behavior coincides with the conductance behavior for $0.5 < q_0 < 1$. Thus the transport properties of SET are periodic in q_0 with the period 1. However, this

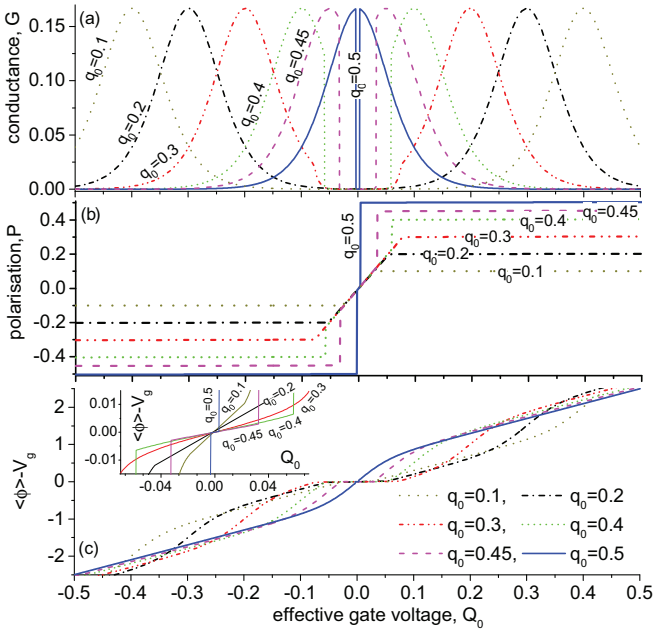

FIG. 4. (Color online) (a) Conductance vs effective gate voltage Q_0. (b) Ferroelectric polarization vs Q_0. (c) Voltage bias in the gate capacitor, $\langle\phi\rangle - V_g$. The jumps in the conductance and polarization in Fig. 3 for $q_0 < 0.5$ are related to a memory effect instability but with a thin hardly detectable hysteresis loop. (Insert) Voltage bias vs Q_0 for small values of Q_0. All parameters are the same as in Fig. 3, except $T = 0.03$.

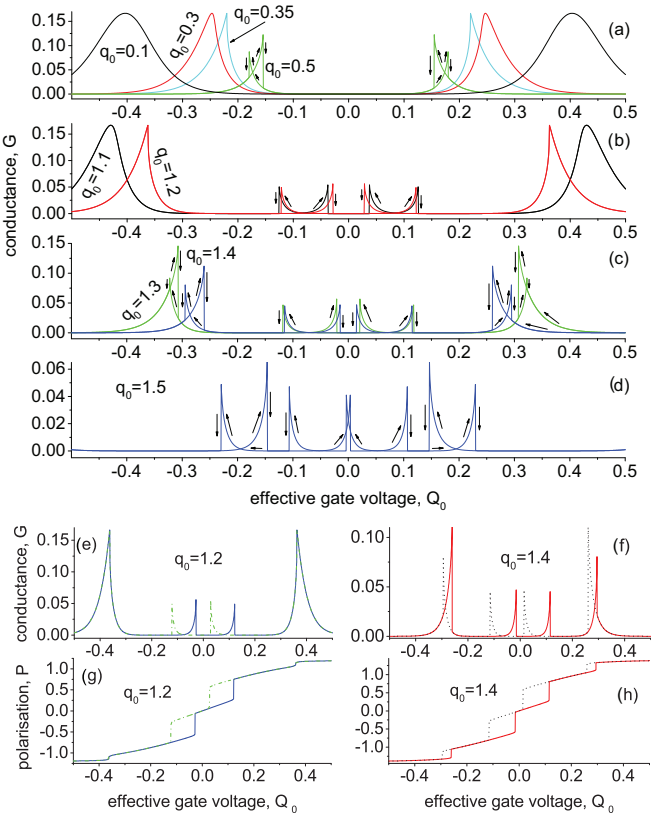

FIG. 5. (Color online) Conductance G and polarization P vs q_0 for $V_s = 1$. All parameters are the same as in Fig. 3, except $T = 0.03$. With increasing q_0 the conductance peaks are shifting towards $Q_0 = 0$. At critical q_0, bifurcation appears and the conductance peaks close to $Q_0 = 0$ become memory dependent. (a) For $q_0 < 0.35$, the conductance $G(Q_0)$ is an ambiguous function. At $q_0 \approx 0.35$, a bifurcation point for the first pair of G peaks appears. (b) At $q_0 \approx 1.2$, the second bifurcation point for the next pair of conductance peaks appears. (c) Evolution of the memory effect with q_0. (d) For further increase of q_0, the memory-dependent conductance peaks are shifting towards $Q_0 = 0$ and finally "collide" with each other. Arrows in (a)–(d) show the memory effect branches for increasing (decreasing) Q_0. (e)–(h) Conductance and polarization of the ferroelectric. The branches of $G(Q_0)$ for increasing (decreasing) Q_0 are shown by solid and discontinuous curves, respectively.

statement is approximate: it is valid for small values of switching voltage V_s and a negligible parameter α only.

The insert in Fig. 4 shows the deviation of $\langle\phi\rangle$ from V_g in the region, $(ne - q_0)/C \lesssim V_g \lesssim (ne + q_0)/C$. It nearly linearly depends on Q_0. After the substitution of $\tanh(\frac{\langle\phi\rangle - V_g}{V_s})$ instead of $\mathrm{sign}(\phi - V_g)$ in Eq. (2), an estimate follows that in the leading order over V_s, $\langle\phi\rangle - V_g \approx V_s Q_0/q_0$.

2. *Ferroelectric with large switching field: $V_s \gtrsim 1$. Breaking and condensation of conductance peaks*

For a large switching field, $V_s \gtrsim 1$, the picture is more complicated. The conductance $G(Q_0, q_0)$ is not a periodic function of parameter q_0 any more. Instead, some interesting effects related to the breaking and condensation of conductance peaks appear.

The closest peaks to $Q_0 = 0$ are not only shifted but also reshaped and finally break at the critical values of parameter q_0, Fig. 5. We classify the conductance peaks by their original positions at $q_0 = 0$ when they are located at half-integer Q_0. We call the peaks located at $Q_0 = \pm 1/2$ the first pair of peaks, while the peaks sitting at $Q_0 = \pm 3/2$ the second pair of peaks. The first pair of conductance peaks breaks at $q_0 = q_0^{c1}$, while the second pair breaks at $q_0^{c2} \gtrsim q_0^{c1}$, Fig. 5. By increasing the parameter q_0, the memory-dependent conductance peaks slowly regroup around $Q_0 = 0$, some of them even "collide" with each other, Fig. 5(d). We call this system behavior the conductance peak condensation.

We introduce the quantity $\alpha_1(V) = \partial P/\partial V$. In the vicinity of zero voltage, $\alpha_1 \approx q_0/V_s$. For voltages $V > V_s$, we find $\alpha_1 \approx 0$. The relation between the grain charge and the grain potential has the form $ne = Q_0 + C_\Sigma\phi + \int_0^{\phi - V_g} \alpha_1(u)du$. The position of conductance peaks can be approximately evaluated using the following relation:

$$Q_0^n + \int_0^{Q_0/C_g} \alpha_1 du = (n + 1/2)e. \tag{7}$$

In the vicinity of $Q_0 = 0$, the distance between peaks reduces from $1e$ to $1e/(1 + \alpha/C_g)$. For $Q_0 > V_s C_g$, the interpeak distance becomes $1e$.

Now we focus on the polarization dependence of parameters Q_0 and q_0 and their correlation with features in the conductance peaks. As follows in Figs. 5(e)–5(h), the polarization also shows a memory effect similar to the conductance. In Fig. 5(g), one can see a number of hysteresis loops; their edges exactly correspond to specific features in the conductance; the

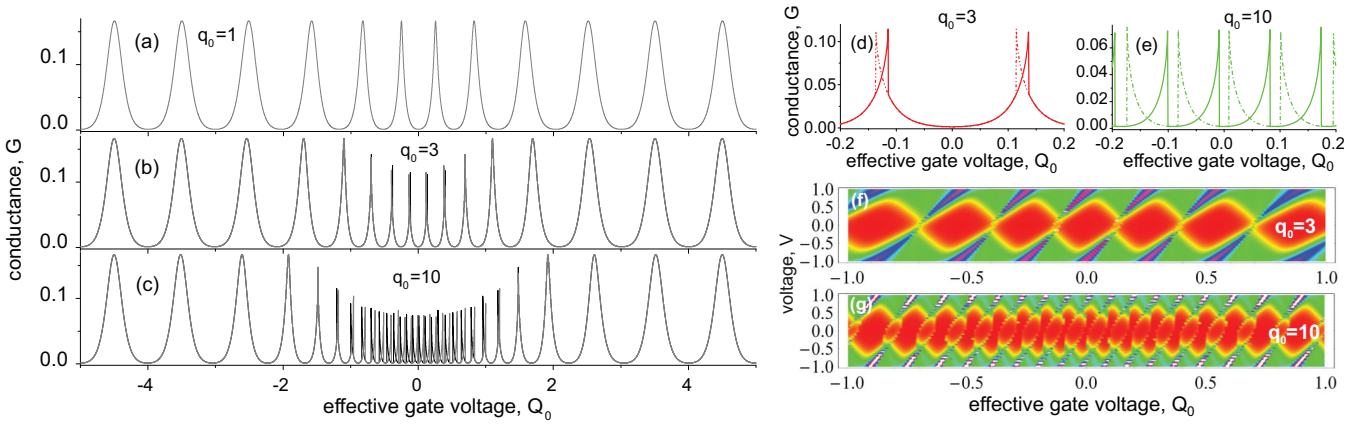

FIG. 6. (Color online) SET device at saturation voltage $V_s = 5$. Parameters are the same as in Fig. 3. (a)–(c) Conductance evolution with $q_0 = 1,3,10$. (d) and (e) Fine structure of the conductance peaks for $q_0 = 3,10$. Branches of $G(Q_0)$ for increasing (decreasing) Q_0 are shown by solid and discontinuous curves. (f) and (g) Conductance density plots; the Coulomb island-structures strongly differ from the SET without ferroelectricity.

number of the hysteresis loops corresponds to the number of conductance peaks broken and "condensed" near $Q_0 = 0$. At first glance, the sharp changes in the polarization in Fig. 5 contradict the chosen parameter $V_s = 1$ that makes the polarization a smooth function, Eq. (1). However, the features are related to the quantization of the excess charge on the grain of SET and not to the parameter V_s.

In the vicinity of Q_0^n, the ground state of the SET is described by Eqs. (A21)–(A23). These equations provide the criterion for the hysteresis appearance:

$$T < T_{\rm cr}^n = \frac{E_c^0 \alpha_1}{4\left[C_\Sigma - \alpha_1\left(Q_0^n/C_g\right)\right]}. \qquad (8)$$

The hysteresis appears first for peaks in the vicinity of $Q_0 = 0$ where α_1 is large. At large Q_0 the hysteresis disappears since $\alpha_1 \to 0$. Similar to steplike polarization behavior the hysteresis disappears with increasing temperature.

In Fig. 6, we investigate an SET with a large switching voltage, $V_s = 5$. Qualitatively, the conductance behavior is similar to the case of $V_s = 1$ except the fact that more conductance peaks are involved in the memory effect for similar values of q_0. Figure 6 shows the evolution of conductance with parameter $q_0 = 1,3,10$. The density plots for conductance show a complicated structure, strongly nonperiodic in Q_0 unlike the SET without ferroelectricity.

Analyzing the numerical data, we conclude that the conductance peaks condensation appears for the following gate voltages: $|V_g| - \langle\phi\rangle_{\max} < V_s$ or $|Q_0| < C_g(V_s + \langle\phi\rangle_{\max})$, where $\langle\phi\rangle_{\max}$ is the maximum grain potential. At zero temperature, $T = 0$, the maximum grain potential is $\langle\phi\rangle_{\max} = \frac{|e|}{2C_\Sigma}$. The number of condensed peaks is approximately equal to the maximum polarization charge that the ferroelectric can induce on the grain, $N_{\rm cond} \approx 2q_0$.

3. *Temperature dependence of the memory effect*

The important question is the temperature dependence of the memory effect. According to Eq. (5), the width of the conductance peaks in an SET without ferroelectricity is approximately proportional to the temperature. A similar effect can be seen with a ferroelectric located in the gate capacitor, see Fig. 7(a). Moreover, it follows that there is a pronounced temperature dependence of the critical q_0 where the first, second, etc., peaks undergo the bifurcation and acquire the

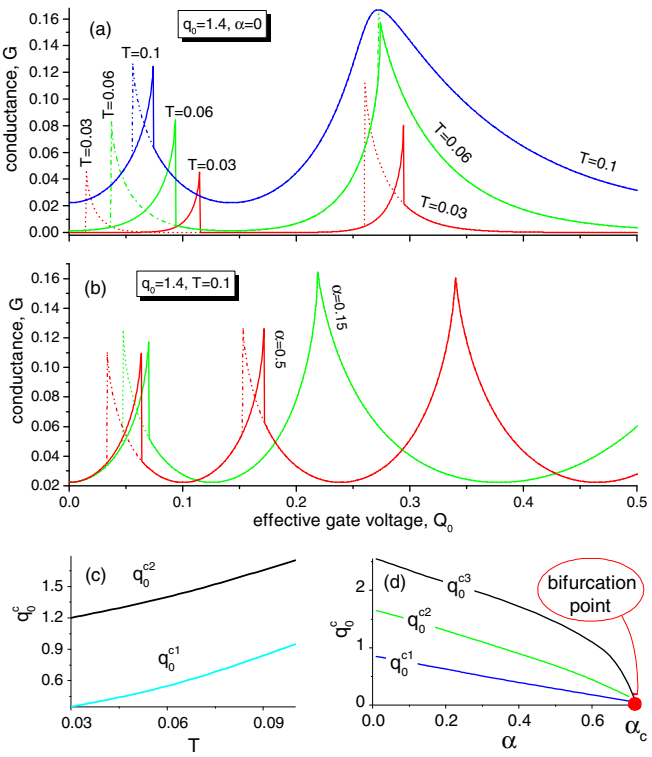

FIG. 7. (Color online) (a) and (b) Memory effect in the conductance for different temperatures and parameters α. All parameters are the same as in Fig. 3, except $V_s = 1$. Branches of $G(Q_0)$ for increasing (decreasing) Q_0 are shown by solid and discontinuous curves. (c) and (d) Critical q_0 where the first and the second pairs of conductance peaks undergo the bifurcation and acquire a memory dependence. (c) Suppression of q_c^0 for finite α. (d) Bifurcation point α_c where all q_c^0 merge and go to zero. The conductance $G(Q_0)$ behavior for $\alpha > \alpha_c$ is different from its behavior for $\alpha < \alpha_c$.

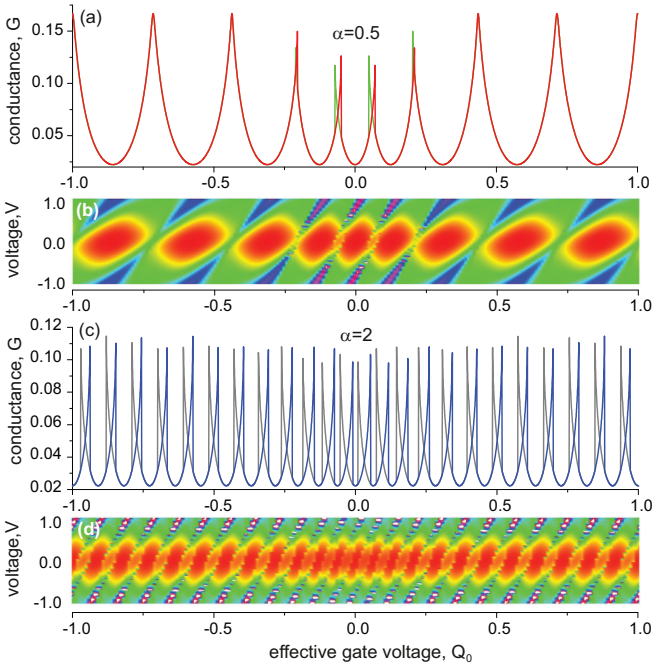

FIG. 8. (Color online) Conductance $G(Q_0)$ behavior for $\alpha > \alpha_c$ is different from its behavior for $\alpha < \alpha_c$. Since all q_c are zero above α_c, the conductance peaks have hysteresis for all Q_0. Here, $V_s = 1$, $T = 0.1$, $q_0 = 1$, $\alpha = 0.5 < \alpha_c$ in (a) and (b), while $\alpha = 2 > \alpha_c$ in (c) and (d). Branches of $G(Q_0)$ for increasing (decreasing) Q_0 are shown in (a), in red and green curves [in (b), in blue and grey curves].

memory dependence. The graphs of $q_0^{c1,2}$ are shown in the inset of Fig. 7(c).

4. *Influence of finite linear term in Eq. (1)*

The presence of the linear term α in Eq. (1) for a polarization P strongly influences the conductance of an SET, Fig. 7(b). Generally, a finite α leads to the renormalization of α_1: $\alpha_1 \to \alpha_1 + \alpha$. Finite α causes the hysteresis behavior of all peaks at small enough temperature. The presence of a small α shifts the conductance peaks and reduces their amplitudes, while the larger α changes the critical values of parameter q_0 where the corresponding conductance peaks undergo a bifurcation and acquire a memory dependence. Figure 7(d) shows that the presence of a finite α suppresses q_c^0. There is a bifurcation point α_c where all q_c^0 merge and reach zero. The behavior of conductance $G(Q_0)$ for $\alpha > \alpha_c$ is very different from its behavior for $\alpha < \alpha_c$. This is related to the fact that all q_c are zero above α_c therefore all the conductance peaks for any value of parameter Q_0 have the hysteresis, Fig. 8.

The critical α can be found analytically. We find α corresponding to an ambiguous solution for the ferroelectric polarization q_e in the limit $Q_0 \to \infty$ using the self-consistency equation $q_g = q_g(V) = q_g(\langle\phi\rangle(Q_0 + q_g) + Q_0/C_g)$, Appendix. Differentiating in voltage Q_0 we find

$$\frac{dq_g}{dQ_0} = \alpha\left[\frac{d\langle\phi\rangle(Q_0')}{dQ_0'}\left(1 + \frac{dq_g}{dQ_0}\right) + \frac{1}{C_g}\right], \qquad (9)$$

where $Q_0' = Q_0 + q_g$ and $\langle\phi\rangle(Q_0)$ denotes the average potential of an SET without a ferroelectric in the gate capacitor. The ambiguity in the solution of $q_g(Q_0)$ results in the appearance of singularity in its derivative. According to Eq. (9), the derivative dq_g/dQ_0 becomes singular at some points if

$$\max_{Q_0}\left(\alpha\frac{d\langle\phi\rangle(Q_0)}{dQ_0}\right) > 1. \qquad (10)$$

According to the orthodox theory, the derivative of the average potential approaches its maximum at the degeneracy points leading to

$$\alpha_c = C_\Sigma\left(\frac{E_c}{2T} - 1\right)^{-1}. \qquad (11)$$

Another effect due to the presence of finite α is the renormalization of the distances between the conductance peaks for Q_0 away from zero. For zero temperature, the distances between peaks are reduced by a factor of $(1 + \frac{\alpha}{C_g})/(1 + \frac{\alpha}{C_\Sigma})$.

5. *Giant hysteresis memory loop in the absence of $P(V)$ hysteresis ($V_h = 0$)*

Above, we showed that ferroelectricity drives the memory effect. Here, we show that it can be "giant." This is so if the effective charge "induced" by the ferroelectric at the grain is large enough, for example, $q_0 = 10$, Fig. 9. We mention that we still use $V_h = 0$ such that the hysteresis in $P(\mathcal{E})$ is absent, Eq. (1). However, $P(Q_0)$ has a large hysteresis. Each small step in $P(Q_0)$ curve in Fig. 9(b) corresponds to the change of the grain charge by the charge quantum. This large Coulomb blockage hysteresis is further increased for $V_h > 0$. This giant hysteresis memory loop has potential for applications in memory devices.

This effect can be thought of as an extreme case of "peak condensation." When enough peaks are "condensed," the conductance behavior acquire the quasioscillatory character in the vicinity of $Q_0 = 0$. Physically, this corresponds to the situation when a small change in Q_0 causes the number of electrons on the grain to be changed by one at the expense of the FE polarization. As a result of being a periodic function of the number of excess electrons on the grain the conductance changes little in this process. The same is true for the average potential.

Below we discuss the SET parameters and conditions to observe the effect of gigantic hysteresis loop. First, the width of the hysteresis loop is restricted by the gate capacitance C_g meaning that it is beneficial to have a large C_g, $C_g > C_1, C_2$. Second, the switching voltage V_s should be of the order of 1 for the polarization not to flip to fast with the change of Q_0. Third, the conductance peaks should start merging meaning that there should be enough number of them (large q_0) and their width should be sufficient (not too low temperatures, T).

B. Ferroelectric with finite hysteresis loop

Now, we consider a ferroelectric with finite hysteresis in the polarization—the electric field dependence is given by Eq. (1). In general, the state of FE depends on the whole history of its evolution, however, here we consider only processes with a monotonous change of FE polarization where the hysteresis-loop approximation is valid.

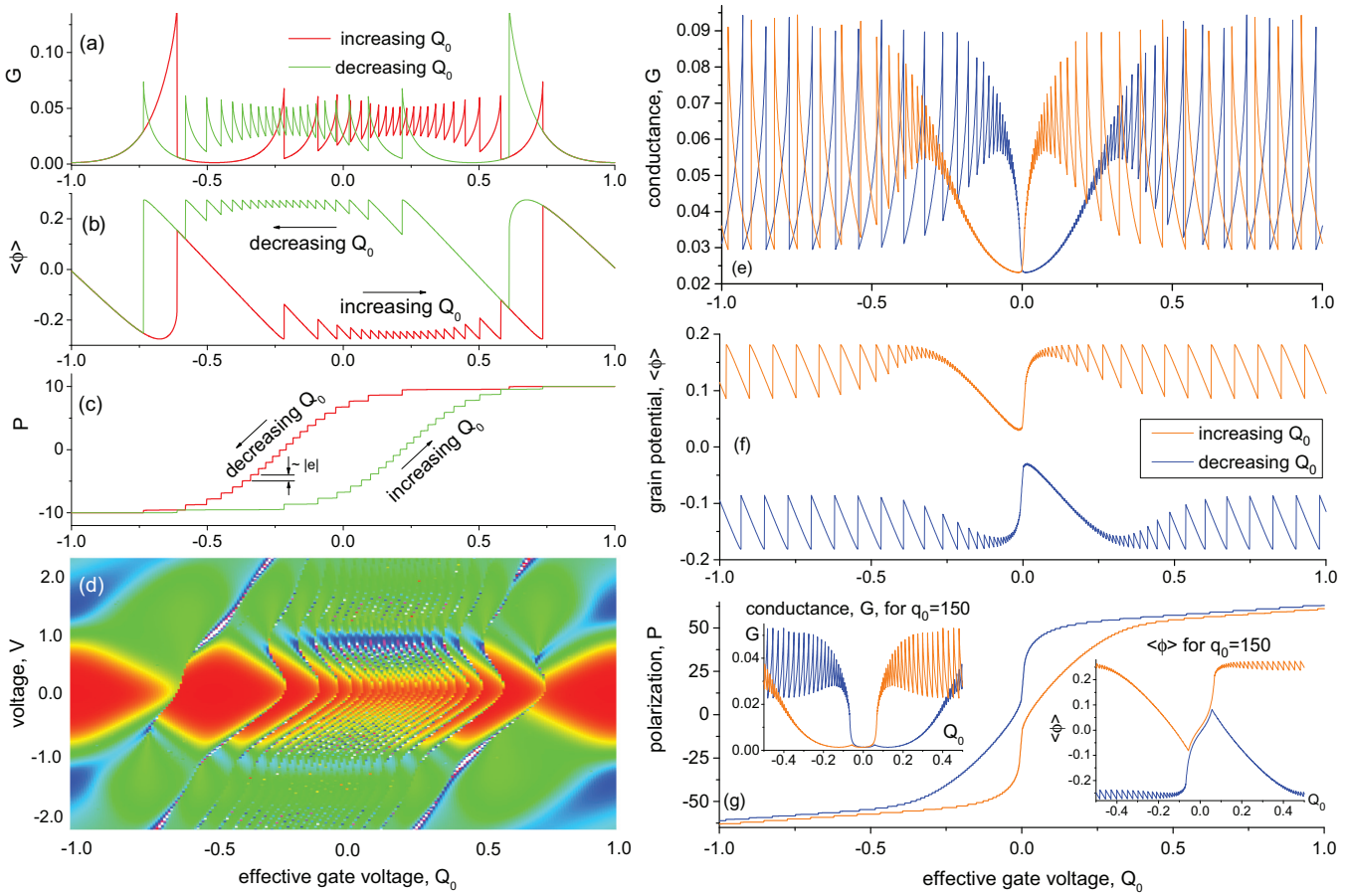

FIG. 9. (Color online) Coulomb blockade induced memory effect [in the absence of $P(V)$ hysteresis]. Here, V_h=0, $C_1 = 0.1$, $C_2 = 0.05$, $C_g = 0.85$, $q_0 = 10$, $T = 0.06$, $V_s = 0.3$, and $\alpha = q_0/(30V_s)$. There is no hysteresis in $P(\mathcal{E})$, see Eq. (1). (a) Conductance, (b) average grain potential (each small step in polarization $P(Q_0)$ in (b) corresponds to the change of the grain charge by the charge quantum), (c) polarization, and (d) Coulomb-diamond plot (color gradients show the conductance). In (a)–(c), the red curves correspond to the memory branch with increasing Q_0, while the green curve to the decreasing Q_0. (d) corresponds to increasing Q_0. Plot (e)–(g) shows the conductance, average potential of the grain and polarization for $q_0 = 50$ and $T = 0.1$ (α here is larger α_c). Insets in (g) show G and $\langle\phi\rangle$ for $q_0 = 150$.

Figure 10 shows the conductance and polarization of a ferroelectric with a finite width hysteresis loop. Graphs (a), (b), and (d) compare SETs with voltages $V_h = 0$ and $V_h > 0$, where for $V_h = 0$ there is no memory effect in the conductance $G(Q_0)$. As follows, the intrinsic hysteresis in the FE polarization-voltage dependence increases the hysteresis in the conductance.

This behavior is predictable in comparison to the negligible hysteresis case. The hysteresis in Eq. (1) is equivalent to the introduction of an additional polarization-induced charge on the grain, where charge is being dependent on the evolution of Q_0:

$$\delta q_g^{\leftrightarrows} = q_0 \left[\tanh\left(\frac{V \pm V_h}{V_s}\right) - \tanh\left(\frac{V}{V_s}\right) \right]. \qquad (12)$$

This additional charge vanishes in the limit $Q_0 \to \pm\infty$, but even in this limit it causes further retardation of the FE polarization change with Q_0 in the region around zero. Moreover, the intrinsic FE polarization causes broadening of the interval of Q_0 where the state of the FE SET is not unique. This interval region is estimated as $|Q_0| < C_g(V_s + \langle\phi\rangle_{\max} + V_h)$.

IV. DISCUSSION

Typical experimental parameters of SETs and ferroelectric materials were discussed in details in our previous paper [15].

A. Influence of cotunneling

Above, we discussed an SET with a ferroelectric gate using the orthodox theory. Now, we go beyond this theory and show how the finite junction conductances influence our results. In particular, we show that the next order corrections to the SET conductance and the island occupation number do not qualitatively change the system behavior, but rather introduce some quantitative corrections.

The orthodox theory assumes that the junction conductances are small compare to $4\pi^2 e^2/h$ and takes into account only the lowest order processes in the tunneling matrix elements. In this section, we use the results of [24] to calculate the second-order corrections to the conductance and the first-order correction to the electron mean occupation number on the island. The latter results in a corrected average island potential $\langle\phi\rangle$ that is used in the self-consistency equation.

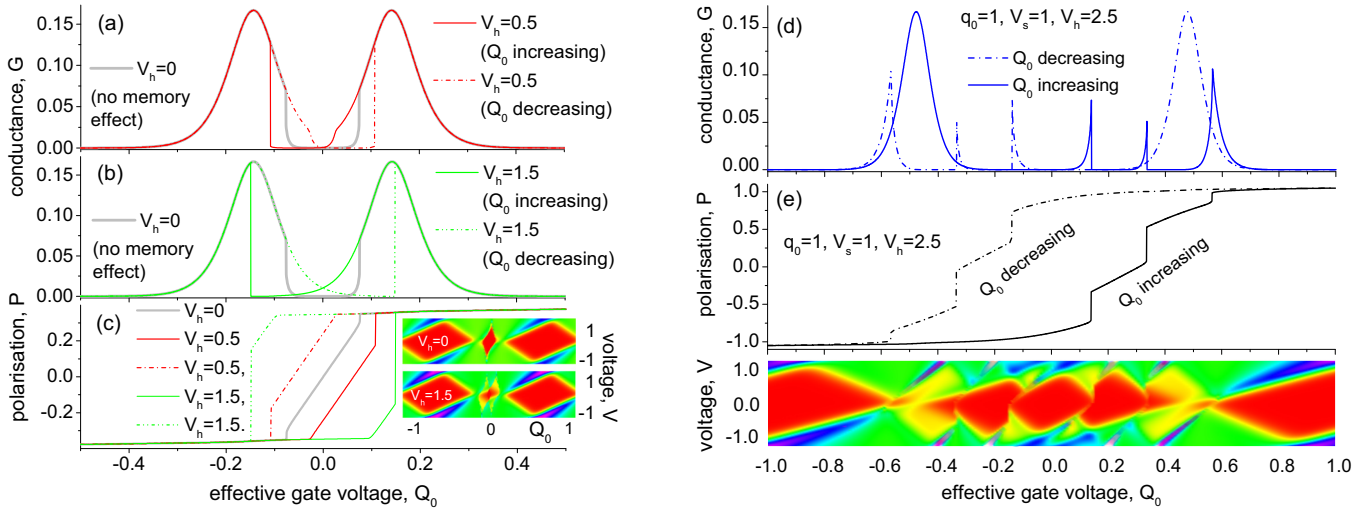

FIG. 10. (Color online) Conductance and polarization of a ferroelectric with finite hysteresis. Graphs (a), (b), and (d) compare SETs with $V_h = 0$ and $V_h > 0$; for $V_h = 0$, the memory effect is absent in $G(Q_0)$. In graphs (a)–(c), parameters $T = 0.03$, $V_s = 0.01$, and $q^0 = 0.35$ are the same as in Fig. 3. As follows from (a)–(c), the hysteresis in the polarization-voltage dependence drives the hysteresis in the conductance. Insets in graph (c): conductance diamonds evolution with voltage V_h. Graphs (d)–(f) show a memory effect in $G(Q_0)$ for $V_h = 0$.

In this section, we measure the resistance in quantum units $R_q = h/(4\pi^2 e^2)$.

In the theory of SET the second-order corrections in the tunneling conductance manifest themselves in reshaping the conductance peaks and in fluctuations of the electron number on the island. For an SET with a ferroelectric gate, the first effect remains, except the fact that the reshaping becomes more complicated in the vicinity of $Q_0 = 0$. However, the quantum charge fluctuations introduce a new effect—they reduce the polarization hysteresis loop. This phenomenon stems from the fact that additional fluctuations of the island charge allow the FE polarization to be switched more easily. However, this effect cannot eliminate the hysteresis completely because the charge fluctuations are suppressed outside the conductance peaks. Typical shifts in the polarization hysteresis due to quantum fluctuations are shown in Fig. 11.

B. Memory-effect devices

The presence of hysteresis in the transport characteristics of ferroelectric SETs has potential applications for memory devices. The memory bit is associated with the particular direction of the ferroelectric polarization in the gate capacitor. The memory storage corresponds to the zero gate voltage ($Q_0 = 0$). For example, if we measure the conductance at a fixed parameter $Q_0 = 0.5$ in Fig. 10(d), it gives the direction of the polarization. This is the reading operation. The writing information (fixation of a particular polarization direction) can be performed by applying a large enough gate voltage (Q_0).

The stored information may be strongly influenced by the fabrication-dependent SET parameters such as q_0 and V_s. For instance, a change in q_0 by half of the elementary charge would shift the conductance peaks by half a period, dramatically changing the relationships between conductances and island potentials for opposite FE polarization.

For memory application, a VDF-TrFE ferroelectric can be used [25]. It has a Curie point above the room temperature. The polarization of this relaxor in the vicinity of room temperature is about $P = 3$ mkmC/m^2 producing a charge $q_0 \approx 0.5$e for 5-nm grain size. Moreover, the magnitude of VDF-TrFE polarization can be tuned varying the VDF concentration. The dielectric permittivity of this relaxor is rather small in the vicinity of room temperature, $\epsilon^{\mathrm{VDF-TrFE}} \approx 5$. Therefore this ferroelectric can not suppress the Coulomb blockade effect and the charging energy can be as high as 2000 K. This allows the memory device to operate at room temperature. For a memory device, the FE thickness can be of order 10 nm. Assuming that the distance between the grain and the leads is about 1 nm, we obtain a good relation between the gate capacitance and the leads capacitors. The switching field of this FE is about 600 kV/cm giving $V_h \approx 2.5$. Using the above estimates one can see that the SET with a VDF-TrFE ferroelectric has a behavior similar to the one shown in Fig. 10. Therefore this system can be used for memory applications.

However, utilizing the giant hysteresis memory loop described in Sec. IIIA5 can provide another configuration, which is less sensible to the SET parameters. As numerical calculations show (see Fig. 11), for a large enough parameter q_0, the island potential tends to "stick" to its maximum or minimum value at $Q_0 = 0$ depending on the way it was set there. Thus the island potential may serve as a reliable indicator of the ferroelectric polarization, which can be directly measured using an auxiliary quantum dot [26].

C. Conclusions

We investigate the electron transport properties of an SET with an FE insulator placed between the metallic grain and the gate electrode. The mutual influence of charged grain and the FE polarization leads to drastic changes in the SET transport. In particular, (i) there is an ambiguity in the $I(V)$ characteristics of an SET with a ferroelectric gate capacitor originating from the nonlinear mutual influence of electrons at the metallic grain and the FE polarization. It appears even

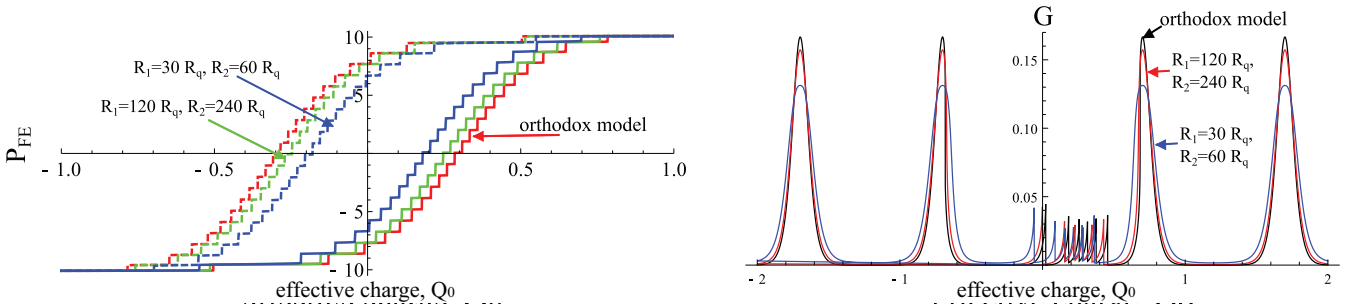

FIG. 11. (Color online) (Left) Coulomb-blockade induced hysteresis loop of the gate ferroelectric polarization for different resistances of the tunnel junctions (the polarization is expressed in charge units). (Right) Conductance peaks line shape distortion for different resistances of tunnel junctions (G is normalized to the conductance of orthodox model). Parameters: $C_1 = 0.05$, $C_2 = 0.1$, $C_g = 0.85$, $q_0 = 10.1$, $V_s = 0.3$, and $T = 0.03$.

in the absence of hysteresis in the FE polarization. (ii) The state of an SET is no longer periodic in the gate voltage (Q_0). In particular, a "condensation" of the conductance peaks appears in the vicinity of $Q_0 = 0$. The range of Q_0 where the conductance peaks condensate depends weakly on the ferroelectric properties and other transistor parameters. For $V_h = 0$, the peak condensation appears for gate voltages $|V_g| - \langle\phi\rangle_{\max} < V_s$ or $|Q_0| < C_g(V_s + \langle\phi\rangle_{\max})$, where $\langle\phi\rangle_{\max}$ is the maximum grain potential. At zero temperature, $T = 0$, the maximum potential is $\langle\phi\rangle_{\max} = \frac{|e|}{2C_\Sigma}$. The number of the condensed peaks is approximately equal to the maximum polarization charge that the ferroelectric can induce on the grain: $N_{\text{cond}} \approx 2q_0$. (iii) The linear part of the ferroelectric polarization αV substantially influences the conductance behavior as a function of the parameter Q_0. In particular, a finite α leads to the reduction of conductance peaks and the distances between the peaks in the whole range of Q_0 (not only for small Q_0). (iv) A finite hysteresis loop of the FE polarization makes the distinction between forward and backward change of voltage V_g more pronounced. A finite voltage V_h is not needed for ambiguity in the SET state to appear.

ACKNOWLEDGMENTS

N.C. acknowledges the hospitality of Laboratoire de Physique Théorique, Toulouse and CNRS, where this work was finalized, and SIMTECH Program, New Centure of Superconductivity: Ideas, Materials and Technologies (Grant No. 246937). S.F. and A.K. were supported by Russian National Foundation (Grant No. RNF 14-12-01185), N.C. was supported by the Russian Foundation for Basic Research (Grant No. 13-518 02-0057a), and I.B. was supported by the NSF under Cooperative Agreement Award No. EEC-1160504, NSF Award No. DMR-520 1158666, and the NSF PREM Award.

APPENDIX: THEORY OF FERROELECTRIC SINGLE-ELECTRON TRANSISTOR

1. Self-consistent solution

In this section, we show how the influence of ferroelectric polarization can be included into the theory of SET. We limit our consideration to the case of sufficiently slow ferroelectric response times τ_P compare to the electron tunneling time $\tau_e = R_\Sigma C_\Sigma$. The opposite limit is discussed in Ref. [15]. We consider the steady-state solutions.

We use the following Hamiltonian to describe the SET:

$$H = H_1 + H_2 + H_I + H_c + H_T. \tag{A1}$$

Here, $H_k = \sum_l \epsilon_{kl} a_{kl}^\dagger a_{kl}$, $k = 1,2,I$ denotes Hamiltonians for isolated right and left leads and the island, respectively, H_T is the tunneling Hamiltonian, and H_c is the Coulomb energy of the form

$$H_c = \frac{1}{2C_\Sigma}\left[e\hat{n} - Q_0 - (C_1 - C_2)\frac{V}{2}\right]^2. \tag{A2}$$

$Q_0 = -C_g V_g$ is the effective charge. The notations for voltages and capacitances are similar to Fig. 1.

The Coulomb Hamiltonian in Eq. (A2) treats the dielectric polarizations in the junctions as classical variables. Thus it can be easily generalized to the case of an additional FE polarization P by adding the term $\propto \hat{n}P$:

$$H_c' = \frac{1}{2C_\Sigma}\left[e\hat{n} - Q_0 - q_g - (C_1 - C_2)\frac{V}{2}\right]^2. \tag{A3}$$

Equation (A3) is valid for "frozen" FE polarization, meaning that it is constant on the time-scales of tunneling. This limit is justified assuming that the slow polarization is defined by the mean field and is weakly influenced by the fast field fluctuations of the charge tunneling. To find a steady state of a SET, the equilibrium FE polarization P_{eq} must be taken constant for calculating the electron tunneling rate. This constant polarization yields an additional constant charge on the island q_g:

$$q_g = \int_g d\mathbf{S}_g \cdot \mathbf{P}_{\mathbf{eq}}. \tag{A4}$$

The Coulomb Hamiltonian in Eq. (A3) coincides with the usual SET Hamiltonian if we introduce a new effective gate charge $Q_0' = Q_0 + q_g$. Thus, for a given FE polarization, the steady state of the FE SET can be calculated using the theory of usual SET. On the other hand, the polarization of the FE by itself is determined by the mean electric field resulting from the microscopical tunneling dynamics. Therefore the complete steady-state solution for the FE SET is obtained when the equilibrium FE polarization and the tunneling dynamics are calculated self-consistently [15].

2. First-order theory

Here, we discussed the first-order perturbation theory in tunneling. For the FE induced charge, we use the following expression:

$$q_g = q_0 \tanh\left(\frac{V \pm V_h}{V_s}\right) + \alpha V. \tag{A5}$$

Here, $V = \langle\phi\rangle - V_g$ is the voltage across the gate junction. The average island potential $\langle\phi\rangle$ that plays a key role in determining the FE polarization is a linear function of the average island occupation number $\langle n\rangle$:

$$\langle\phi\rangle = \frac{1}{C_\Sigma}\left[e\langle n\rangle - Q_0 - q_g - (C_1 - C_2)\frac{V}{2}\right]. \tag{A6}$$

In the leading order, the probability per unit time to change the island occupation number from n to $n \pm 1$ through the first junction is given by the Fermi golden rule:

$$\Gamma^{(1)}_{n\to n\pm1} = \frac{1}{e^2 R_1}\cdot \Delta F_1^{n\to n\pm1} N_B\left(\Delta F_1^{n\to n\pm1}\right), \tag{A7}$$

where $N_B(\omega) = 1/[\exp(\omega/T) - 1]$ is the Bose function [27], R_1 is the tunneling bare resistance, and $\Delta F_1^{n\to n\pm1}$ denotes the free energy change with Q_0' being the effective charge:

$$\Delta F_1^{n\to n\pm1} = \frac{e^2}{C_\Sigma}\left[\frac{1}{2} \pm \left(n - \frac{Q_0'}{e}\right) \pm \frac{(C_2 + C_g/2)V}{e}\right]. \tag{A8}$$

The flow rates defined the probabilities p_n to find n excess electrons on the island through the detailed-balance equations:

$$p_n\left(\Gamma^{(1)}_{n\to n+1} + \Gamma^{(2)}_{n\to n+1}\right) = p_{n+1}\left(\Gamma^{(1)}_{n+1\to n} + \Gamma^{(2)}_{n+1\to n}\right), \tag{A9}$$

with boundary conditions $p_{\pm\infty} = 0$. In their turn, the probabilities p_n are used to calculate the average occupation number and the average potential through Eq. (A6). The last step is to solve Eqs. (A5) and (A6) together to obtain a self-consistent solution.

Knowing the FE induced charge q_g^{eq}, the current through the SET can be found:

$$I = |e| \sum_n p_n\left(\Gamma^{(1)}_{n\to n+1} - \Gamma^{(1)}_{n\to n-1}\right), \tag{A10}$$

where all the rates are calculated with $Q_0' = Q_0 + q_0^{\rm eq}$ being the effective charge.

3. Higher-order corrections

Here, we consider next order corrections to the average occupation number and to the tunneling current. If the corrections for SET without FE are known as a function of the effective charge Q_0, these corrections can be generalized for FE SET. Indeed, to solve the self-consistency Eqs. (A5) and (A6), we need to know the dependence of $\langle n\rangle$ on Q_0 for an SET without ferroelectricity. If this dependence is known, $\langle n\rangle(Q_0) = \langle n\rangle^{(0)}(Q_0) + \langle n\rangle^{(1)}(Q_0) + \ldots$, it can be placed in Eq. (A6) with the proper substitution for $Q_0 \to Q_0 + q_g$.

In the Sec. IV A, we used the results of Ref. [24] for low temperatures, where it was shown that in the first-order theory, the occupation probabilities of only two neighboring states (n and $n+1$ excess electrons) significantly deviate from zero. The correction to the average occupation number is given by

$$\langle n\rangle^{(1)} = \frac{C_\Sigma}{e}\frac{\partial}{\partial Q_0}\left[p_n^{(0)}(\phi_n - \phi_{n-1}) + p_{n+1}^{(0)}(\phi_{n+1} - \phi_n)\right], \tag{A11}$$

where

$$\phi_n = \sum_{k=1,2}\frac{R_q}{R_k}\Delta F_k^{n\to n+1}\,\mathrm{Re}\,\Psi\left[i\frac{\Delta F_k^{n\to n+1}}{2\pi T}\right], \tag{A12}$$

$p^{(0)}_{n,n+1}$ are the lowest-order state occupation probabilities, $R_q = h/(4\pi^2 e^2)$, k denotes junctions, and Ψ is the digamma function.

Following Ref. [24], we introduce the generalized flaw rates to calculate the corrections to the tunneling current:

$$g_k^{\pm}(\omega) = \pm\frac{R_q}{R_k}\frac{\omega - \mu_k}{\exp(\pm(\omega - \mu_k)/T) - 1}, \tag{A13}$$

$$g^{\pm}(\omega) = \sum_{k=1,2} g_k^{\pm}(\omega), \quad g(\omega) = \sum_{\sigma=\pm} g^{\sigma}(\omega), \tag{A14}$$

where $\mu_k = \pm eV/2$ are the chemical potentials of the electrodes. Additionally,

$$\Delta_n = \langle n+1|H_c'|n+1\rangle - \langle n|H_c'|n\rangle. \tag{A15}$$

We consider the case with 0 or 1 excess electrons occupying the island. To calculate the corrections for arbitrary voltages and FE polarization, we shift the parameter Q_0' by $n_{\rm sh}e$, where

$$n_{\rm sh} = \left[\frac{Q_0 + q_g + (C_1 - C_2)V/2}{e}\right]. \tag{A16}$$

Therefore, in the following, we assume that $0 < (Q_0' + (C_1 - C_2)V/2)/e < 1$. The first-order tunneling current can be written as follows:

$$I^{(1)}(\Delta_0) = \frac{4\pi^2 e}{h}\frac{g_2^+(\Delta_0)g_1^-(\Delta_0) - g_1^+(\Delta_0)g_2^-(\Delta_0)}{g(\Delta_0)}. \tag{A17}$$

The second-order contribution to the tunneling current is divided into three parts: $I^{(2)}(\Delta_0) = \sum_{i=1}^3 I_i^{(2)}(\Delta_0)$, where

$$I_1^{(2)}(\Delta_0) = \int d\omega\, I^{(1)}(\omega)g(\omega) \times \mathrm{Re}\left[p_0^{(0)}R_-(\omega)^2 + p_1^{(0)}R_+(\omega)^2\right], \tag{A18}$$

$$I_2^{(2)}(\Delta_0) = -I^{(1)}(\Delta_0)\int d\omega\,\mathrm{Re}\sum_{\sigma=\pm} g^{\sigma}R_{\sigma}(\omega)^2, \tag{A19}$$

$$I_3^{(2)}(\Delta_0) = -\frac{\partial I^{(1)}(\Delta_0)}{\partial\Delta_0}\int d\omega\,\mathrm{Re}\sum_{\sigma=\pm} g^{\sigma}R_{\sigma}(\omega), \tag{A20}$$

where $R_\pm(\omega) = 1/(\omega - \Delta_0 + i0^+) - 1/(\omega - \Delta_{\pm1} + i0^+)$ and the poles at $\omega = \Delta$ are regularized as Cauchy's principal values $\mathrm{Re}[1/(x + i0^+)] = P\frac{1}{x}$ and their derivatives $\mathrm{Re}[1/(x + i0^+)^2] = -\frac{d}{dx}P\frac{1}{x}$.

4. Choosing branches

The self-consistent solution of Eqs. (A5) and (A6) may not be unique leading to the hysteresis behavior discussed in this paper. Thus we encounter the problem of choosing branches. Here, we explain the rules for selecting the solutions.

The self-consistent state is unique for the effective charge being away from the resonance and the linear part of the FE polarizability α being sufficiently small. There are two situations: (i) Q_0 evolved from $-\infty$ to the right and (ii) from ∞ to the left. Over the course of Q_0 evolution at some values of parameter Q_0 the solution can become discontinuous. In this case, we assume that the polarization "jumps" to the nearest available position. There is no ambiguity in choosing the new state, because the polarization always evolves monotonically and takes its maximum or minimum value depending on the direction of evolution.

5. Ground state of FE SET with steplike polarization

For calculating the ground state of the system, all states are important. However, the hopping probability decreases exponentially with increasing the free energy of a state. Therefore we consider only few states that are the closest to the considered point. The number of these states depends on the parameter q_0 and the considered point. For $q_0 < 0.5e$, only two states n and $n+1$ are important for calculating $\langle\phi\rangle$ for any n. Increasing the parameter q_0 leads to a shift of the energy intersection points to $Q_0 = 0$. For $q_0 > 0.5$, the situation is more complicated. In the vicinity of $Q_0 = 0$, a lot of intersections of different energy branches occur and one has to take into account many different states. However, for large values of Q_0, only two states of energy intersection points are important.

We consider the case when two states are enough to describe the system state and concentrate on the vicinity of the point $Q_0 = e(n+1/2) - q_0$ with $Q_0 > 0$ and $q_0 < 0.5e$. The average charge is given by the expression

$$\langle ne\rangle = \langle Q\rangle = e[nW_n + (n+1)W_{n+1}], \tag{A21}$$

where $W_{n,n+1}$ are the probabilities for the system to be in the state with n and $n+1$ electrons on the grain. If only two states are present, we find

$$\begin{aligned} W_n &= \frac{\Gamma_{n,n+1}}{\Gamma_{n,n+1}+\Gamma_{n+1,n}},\\ W_{n+1} &= \frac{\Gamma_{n+1,n}}{\Gamma_{n,n+1}+\Gamma_{n+1,n}},\\ \Gamma_{n,n+1} &= \frac{E_c^0(n+1/2-Q_0/e-S\,P(\langle\phi\rangle-V_g)/e)}{e^{\beta E_c^0(n+1/2-Q_0/e-S\,P(\langle\phi\rangle-V_g)/e)}-1},\\ \Gamma_{n+1,n} &= \frac{-E_c^0(n+1/2-Q_0/e-S\,P(\langle\phi\rangle-V_g)/e)}{e^{-\beta E_c^0(n+1/2-Q_0/e-S\,P(\langle\phi\rangle-V_g)/e)}-1}, \end{aligned} \tag{A22}$$

where $\beta = T^{-1}$ and the parameter S is approximately the area of the grain in contact with the ferroelectric. Averaging Eq. (3), we find the following relation:

$$\langle Q\rangle = C_\Sigma\langle\phi\rangle + Q_0 + SP(\langle\phi\rangle - V_g). \tag{A23}$$

Equations (A21) and (A23) have always a single solution. Therefore there is no hysteresis in the system for $q_0 < 0.5e$ and arbitrary Q_0. The conductivity of an SET has a maximum at $W_n = W_{n+1}$. These maxima are located at point $Q_0 = e(n+1/2) - q_0$. The average potential at these points is $\langle\phi\rangle = 0$.

For $q_0 > 0.5e$ and $Q_0 > 0.5e$, there is no hysteresis. In the vicinity of $Q_0 = 0$, the system shows a hysteresis and can not be described by two states. For $q_0 \sim 0.5e$, three states $n = 0, \pm 1$ need to be taken into account in the vicinity of $Q_0 = 0$, see Fig. 3. For $q_0 \sim 1.5e$, five states $n = 0, \pm 1, \pm 2$, etc.

For $q_0 \sim 0.5e$, the system probabilities with $n = 0, \pm 1$ have the form

$$\begin{aligned} W_{-1} &= \frac{\Gamma_{0,-1}}{\Gamma_{-1,0}}W_0,\\ W_1 &= \frac{\Gamma_{0,1}}{\Gamma_{1,0}}W_0,\\ W_0 &= \left(1+\frac{\Gamma_{0,-1}}{\Gamma_{-1,0}}+\frac{\Gamma_{0,1}}{\Gamma_{1,0}}\right)^{-1}. \end{aligned} \tag{A24}$$

The average charge $\langle Q\rangle$ is given by the following expression:

$$\langle Q\rangle = e(W_1 - W_{-1}). \tag{A25}$$

Solving Eqs. (A25) and (A23), we find the average potential $\langle\phi\rangle$. Figure 12 shows the dependence Eq. (A25) (solid line) and Eq. (A23) (dashed line) on $\langle\phi\rangle$ for $Q_0 = 0$. In this figure, the curves have three intersections at points $\phi_{-1,0,1}$ meaning that the system has hysteresis. The asymptotic behavior of Eq. (A25) for $Q_0 = 0$ is the following:

$$Q_{\max}(T) = \pm\frac{e\Gamma_{0,1}}{\Gamma_{0,1}+\Gamma_{1,0}}. \tag{A26}$$

The value $Q_{\max}$ depends on temperature and decreases with increasing T. At temperature $T = T_h$, it becomes smaller than q_0. For temperature $T > T_h$, the hysteresis disappears. However, at high enough temperatures, all states need to be taken into account and the description with three states only ($n = 0, \pm 1$) can be incorrect.

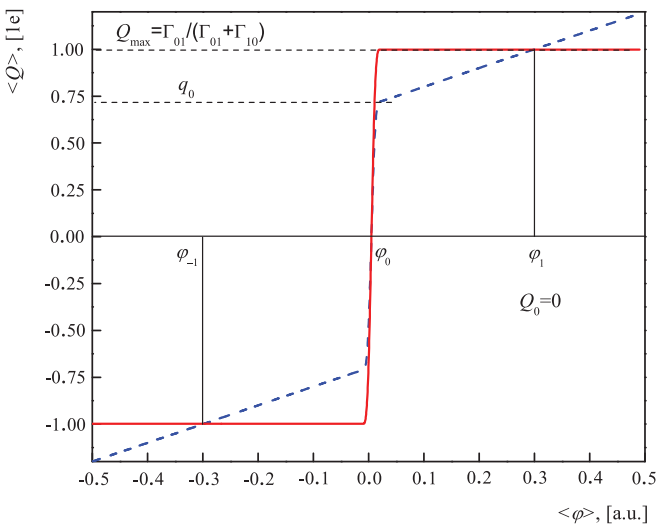

FIG. 12. (Color online) Dependencies of Eq. (A25) (solid line) and Eq. (A23) (dashed line) on $\langle\phi\rangle$. The curves are plotted for the following parameters: $q_0 = 0.55$, $C_g = 0.2$, $T = 0.03$, and $Q_0 = 0$.

[1] M. Dawber, I. Szafraniak, M. Alexe, and J. Scott, J. Phys. C **15**, L667 (2003).

[2] C. Ahn, K. Rabe, and J.-M. Triscone, Science **303**, 488 (2004).

[3] M. Dawber, K. M. Rabe, and J. F. Scott, Rev. Mod. Phys. **77**, 1083 (2005).

[4] L. Wang, J. Yu, Y. Wang, G. Peng, F. Liu, and J. Gao, J. Appl. Phys. **101**, 104505 (2007).

[5] Y.-J. Zhang, T.-L. Ren, and L.-T. Liu, Integr. Ferroelectr. **95**, 199 (2007).

[6] J. F. Scott, Science **315**, 954 (2007).

[7] P. Maksymovych, S. Jesse, P. Yu, R. Ramesh, A. P. Baddorf, and S. V. Kalinin, Science **324**, 1421 (2009).

[8] Y.-H. Chu, L. W. Martin, M. B. Holcomb, M. Gajek, S.-J. Han, Q. He, N. Balke, C.-H. Yang, D. Lee, W. Hu, Q. Zhan, P.-L. Yang, A. Fraile-Rodriguez, A. Scholl, S. X. Wang, and R. Ramesh, Nat. Mater. **7**, 478 (2008).

[9] W. Lee, H. Han, A. Lotnyk, M. A. Schubert, S. Senz, M. Alexe, D. Hesse, S. Baik, and U. Gösele, Nat. Nanotechnol. **3**, 402 (2008).

[10] S. V. Kalinin, A. N. Morozovska, L. Q. Chen, and B. J. Rodriguez, Rep. Prog. Phys. **73**, 056502 (2010).

[11] J. Sinsheimer, S. J. Callori, B. Bein, Y. Benkara, J. Daley, J. Coraor, D. Su, P. W. Stephens, and M. Dawber, Phys. Rev. Lett. **109**, 167601 (2012).

[12] S. J. Callori, J. Gabel, D. Su, J. Sinsheimer, M. V. Fernandez-Serra, and M. Dawber, Phys. Rev. Lett. **109**, 067601 (2012).

[13] N. Ortega, A. Kumar, J. Scott, D. B. Chrisey, M. Tomazawa, S. Kumari, D. Diestra, and R. Katiyar, J. Phys. C **24**, 445901 (2012).

[14] A. Chanthbouala, V. Garcia, R. O. Cherifi, K. Bouzehouane, S. Fusil, X. Moya, S. Xavier, H. Yamada, C. Deranlot, N. D. Mathur, M. Bibes, A. Barthélémy, and J. Grollier, Nat. Mater. **11**, 860 (2012).

[15] S. A. Fedorov, A. E. Korolkov, N. M. Chtchelkatchev, O. G. Udalov, and I. S. Beloborodov, Phys. Rev. B **89**, 155410 (2014).

[16] A. D. Armour, M. P. Blencowe, and Y. Zhang, Phys. Rev. B **69**, 125313 (2004).

[17] N. Nishiguchi, Phys. Rev. B **78**, 085407 (2008).

[18] A. N. Korotkov, Phys. Rev. B **49**, 16518 (1994).

[19] D. Averin and K. Likharev, Mesosc. Phenom. Solids **30**, 173 (1991).

[20] D. V. Averin, A. N. Korotkov, and K. K. Likharev, Phys. Rev. B **44**, 6199 (1991).

[21] M. Devoret and H. Grabert, *Single Charge Tunneling* (New York, Plenum, 1992), Vol. 264.

[22] C. Wasshuber, *Computational Single Electronics* (Springer, Berlin, 2001).

[23] The jumps in the conductance and polarization in Fig. 3 for $q_0 < 0.5$ are also related to the memory effect instability but with a rather thin hysteresis loop.

[24] J. König, H. Schoeller, and G. Schön, Phys. Rev. Lett. **78**, 4482 (1997).

[25] T. Yamada, T. Ueda, and T. Kitayama, J. Appl. Phys. **52**, 948 (1981).

[26] C. F. F. H. Niels Ubbelohde, Christian Fricke and R. J. Haug, Nat Commun. **3**, 612 (2012).

[27] N. M. Chtchelkatchev, A. Glatz, and I. S. Beloborodov, Phys. Rev. B **88**, 125130 (2013).